In vivo prostate cancer research: Key interspecies prostate anatomical features for translation medicine

Elisabete Nascimento-Gonçalves[1,2,3] (iD), Fernanda Seixas[4,5] (iD), Rita Ferreira[3] (iD),
Paula A. Oliveira[1,2] (iD) and Bruno Colaço[4,6*] (iD)

[1]*Centre for the Research and Technology of Agro-Environmental and Biological Sciences (CITAB),
University of Trás-os-Montes and Alto Douro (UTAD), Vila Real, Portugal*
[2]*Institute for Innovation, Capacity Building and Sustainability of Agri-Food Production
(Inov4Agro), UTAD, Vila Real, Portugal*
[3]*LAQV-REQUIMTE, Department of Chemistry, University of Aveiro (UA), Aveiro, Portugal*
[4]*Animal and Veterinary Research Centre (CECAV), Associate Laboratory for Animal and
Veterinary Science—AL4AnimalS, UTAD, Vila Real, Portugal*
[5]*Department of Veterinary Sciences, University of Trás-os-Montes and Alto Douro, Vila Real, Portugal*
[6]*Department of Zootechnics, University of Trás-os-Montes and Alto Douro, Vila Real, Portugal*

Abstract

Prostate cancer (PCa) is a prevalent malignancy affecting men worldwide. Animal models play a crucial role in studying PCa pathology and discovering novel approaches to prevent, detect and treat this disease. However, the challenge of translational medicine is the limited reproducibility and inadequate recapitulation of human conditions in animal models. Therefore, a comprehensive understanding of the macroscopic and microscopic anatomy of the prostate gland among distinct animal species is essential for better translating research findings to clinical practice. This review aims to compare and describe the macroscopic and microscopic anatomy of the prostate gland in humans, rats, and dogs, emphasizing the relevant features. Despite the anatomical differences between these species, rats are a valuable model to study human prostate diseases, once they share some features implicated in carcinogenesis in humans. Dogs, on the other hand, are considered the best model for studying PCa due to the development of spontaneous cancer with a higher incidence when compared with other animals and the development of bone metastases. Moreover, the lymphatic system and the sentinel lymph node role and mapping are similar in dogs and humans. However, it is important to recognize that no animal model can directly mimic all aspects of PCa as the human prostate is anatomically different from that of rats and dogs. Therefore, it is essential to analyze and understand the intra- and interspecies variability when translating research findings into clinical practice. This review highlights the importance of a thorough understanding of the anatomical differences between the prostate gland in humans, rats, and dogs when selecting the appropriate animal model for studying PCa.

Keywords: Anatomy, Dog, Human, Prostate, Rat.

Introduction

Herophilus of Alexandria (335–80 B.C.), a known Greek physician anatomist, described a small male organ located in front of the bladder, named "prohistani" which means "to stand in front of" (Bay and Bay, 2010; Sharma *et al*., 2017). In 1,536, this organ was designated as "prostate" by the Italian anatomist Niccolò Massa (1489–1569), who first described the prostate and its exact location (Palmer, 1981). The prostate is the largest male accessory sex gland and is responsible for the production of 25%–30% of slightly alkaline fluid which constitutes seminal fluid (Sharma *et al*., 2017). However, this gland is not exclusive to males, being present in women and other female mammals, such as Mongolian gerbils (Sanches *et al*., 2016; Biancardi *et al*., 2017).

The prostate may be affected by several disorders, such as prostatitis, prostatic hyperplasia, and cancer. Prostate cancer (PCa) is one of the most worldwide common cancer, affecting in 2020 approximately 1.4 million men (Sung *et al*., 2021).

In literature we can find several *in vivo* models to study PCa, allowing not only the study of basic aspects related to the disease but also its development, the process of metastasis, and the development of new therapeutic approaches (Bosland, 1999; Shirai *et al*., 2000; Roy-Burman *et al*., 2004; Nascimento-Gonçalves *et al*., 2018, 2019, 2020).

The use of laboratory animals is widely used in preclinical studies, and it is assumed that the basic biological processes are sufficient to allow extrapolation

*****Corresponding Author:** Bruno Colaço. Animal and Veterinary Research Centre (CECAV), Associate Laboratory for Animal and Veterinary Science—AL4AnimalS, UTAD, Vila Real, Portugal. Email: *bcolaco@utad.pt*

of results obtained in animal experimentation to human clinical practice. However, there is no perfect animal model that can mimic all stages of disease exactly as it does in humans. Choosing the appropriate animal model for research is critical to ensure the faithful translation of results to humans. Another important aspect is the experimental design which must be rigorous and allow reproducibility of the findings.

Actually, rats and mice are the most used laboratory animals in the PCa field due to their advantages, such as easy of handling and their physiological and genetic similarities to humans (Nascimento-Gonçalves *et al.*, 2019). However, rodents have some limitations as animal models for studying PCa, such as their anatomy, lifespan, and body weight, that may interfere with carcinogenesis (Fagundes and Taha, 2004; Cekanova and Rathore, 2014). The dog is an interesting animal model for PCa due to the anatomical, histopathological, and epidemiological similarities with human PCa (LeRoy and Northrup, 2009; Sun *et al.*, 2017b). For example, dog PCa can develop spontaneously, metastasizes in bone, and lacks NKX3.1 and androgen receptor (AR), just like men (LeRoy and Northrup, 2009; Fonseca-Alves *et al.*, 2018; Laufer-Amorim *et al.*, 2019). On the other hand, there are constraints to the use of dogs in research similar to those carried out with rodents due to ethical issues, difficulties in maintaining these animals in the laboratory, and the long latency period (Pinho *et al.*, 2012).

To improve the translation of preclinical research findings into clinical practice, it is relevant to have a comparative understanding of prostate anatomy in humans and in the most used animals. Although there are several articles and book chapters about prostate anatomy of human (McMinn, 2003; Lee *et al.*, 2011; Bhavsar and Verma, 2014; Sharma *et al.*, 2017; Standring, 2020), rodents (Jesik *et al.*, 1982; Lee and Holland, 1987; Oliveira *et al.*, 2016; Ginja *et al.*, 2019), and dogs (Budras *et al.*, 2007; Smith, 2008; Evans and Miller, 2013; Sun *et al.*, 2017a), as far as authors know there is no single article or book chapter presenting a systematic and exhaustive comparison between them. Thus, our review aims to describe the macroscopic and microscopic anatomy of man, rat, and dog prostate, comparatively, emphasizing the most relevant features for clinical translation.

Macroscopic anatomy
Anatomic structures
The prostate is an accessory gland of the male reproductive system that secretes a prostatic fluid which will constitute the seminal fluid, a component of semen (Jesik *et al.*, 1982; Smith, 2008; Sharma *et al.*, 2017). During ejaculation, the prostate contracts and expels prostatic fluid into the urethra (Seeley *et al.*, 2004). The prostate secretion allows the neutralization of the acidity in testicular and vaginal secretions and is important in the process of transient coagulation of the sperm before this one is released (Seeley *et al.*, 2004).

Anatomically, the rodent prostate is divided into four lobes (cranial, dorsal, lateral, and ventral), named concerning their relative position to the urinary bladder (Fig. 1) (Jesik *et al.*, 1982; Lee and Holland, 1987; Ginja *et al.*, 2019). In both rats and mice, the lobes can be distinguished by their histological characteristics and have different physiological functions, sharing a common clear and gelatinous appearance. Besides that, all lobes are surrounded by a delicate mesothelium-lined capsule and separated from each other by fibrous and adipose connective tissue (Jesik *et al.*, 1982). Although remains a controversial issue, some authors consider
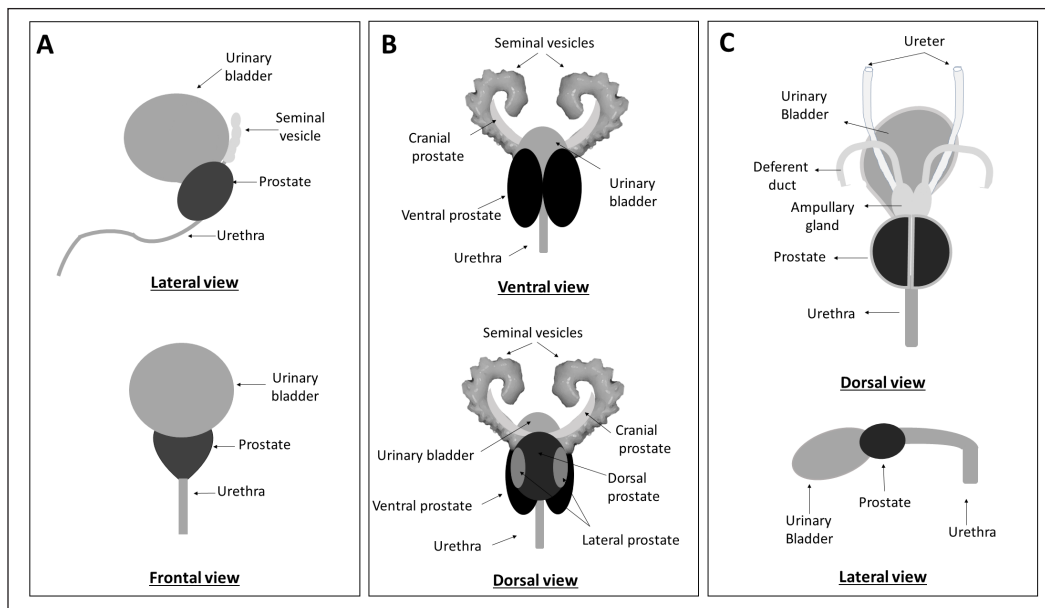

Fig. 1. Schematic representation of macroscopic anatomy of the human (A), rat (B) and dog (C) prostate gland.

the dorsal and lateral prostate (LP) lobes homologous to the human prostate (Shappell *et al*., 2004).

In contrast with the other species described in this review paper, the prostate is the only accessory gland present in the dog reproductive system (Smith, 2008; Evans and Miller, 2013). The dog prostate is a bilobed and ovoid-shaped structure that surrounds the neck of the urinary bladder and the proximal urethra (body and disseminated part of the prostate) (Fig. 1) (Smith, 2008; LeRoy and Northrup, 2009; Cunto *et al*., 2019). The size and weight of the prostate vary with the age, breed, and body weight of the dog (Evans and Miller, 2013). This organ can be considered a mobile organ since its anatomic localization is variable and depends on the age and the bladder distension (Evans and Miller, 2013; Cunto *et al*., 2019); however, the typical localization is the caudal abdomen or the pelvic cavity (Smith, 2008). Until approximately 2 months of age, the prostate is located within the abdominal cavity, from this age until the dog reaches sexual maturity, the prostate is located in the pelvic cavity (Evans and Miller, 2013; Fernando Leis-Filho and Fonseca-Alves, 2019). After sexual maturity, the prostate increases in size and extends cranially into the abdominal cavity (Evans and Miller, 2013; Fernando Leis-Filho and Fonseca-Alves, 2019). The prostate is bounded ventrally by the symphysis pubis, ventral abdominal wall, and dorsally by the rectum (Smith, 2008; Evans and Miller, 2013).

The human prostate is a single lobule structure with a conical shape about the size of a walnut (Bhavsar and Verma, 2014) (Fig. 1), located posterior to the symphysis pubis, anterior to the rectum, and inferior to the urinary bladder, surrounding the proximal urethra (Lee *et al*., 2011; Sharma *et al*., 2017; Ittmann, 2018). A healthy adult prostate weighs around 10–20 g and is grey to reddish according to its activity (Mitterberger *et al*., 2010; Standring, 2020). It is composed of a base, an apex, anterior, posterior, and inferior-lateral surfaces (Lee *et al*., 2011; Bhavsar and Verma, 2014). The base is attached to the neck of the bladder, the apex is located on the superior surface of the urogenital diaphragm that makes contact between the medial surface of the levator ani muscles, the anterior surface is located behind the pubic arch (Sharma *et al*., 2017) and the posterior surface is located on the anterior wall of the rectum, being the posterior surface triangle-shaped and flat (Lee *et al*., 2011; Bhavsar and Verma, 2014). A thin layer of connective tissue, called "Denonvilliers fascia", separates the prostate from the rectum, posteriorly (Sharma *et al*., 2017). The inferior-lateral surface makes the connection between the anterior surface and the rest of the levator ani fascia above the urogenital diaphragm (Lee *et al*., 2011; Bhavsar and Verma, 2014).

Blood supply

Therefore, it is crucial to know the circulation pattern of the prostate in different animal models to better understand the vascularization and possible dissemination route of tumor cells, and the first metastasis's location.

Prostate irrigation derives mainly from the iliac internal artery and its branches. In rats, the internal iliac artery supplies blood to the prostate through the cranial vesical artery, which will supply blood to the different prostate lobes (Jesik *et al*., 1982) (Fig. 2). Moreover, one of their branches, the caudal vesical artery supplies blood to the dorsal surface of the prostate and capsular tissue. The venous blood is returned by the caudal and cranial vesical veins to the internal iliac vein (Jesik *et al*., 1982). The dog prostatic artery, which arises from the internal pudendal artery (branch of the iliac internal artery), is the arterial supply of blood to the dog prostate (Fig. 2) (Budras *et al*., 2007; Smith, 2008; Evans and Miller, 2013). The prostatic artery gives rise to the artery of the ducts deferens and to the caudal vesicular artery (Evans and Miller, 2013). This last artery sends branches to the ureter and urethra and goes toward the urinary bladder (Evans and Miller, 2013). The prostatic artery continues caudoventrally, and before ramifying on the surface of the prostate, gives rise to the small middle rectal artery (Fernando Leis-Filho and Fonseca-Alves, 2019). These branches penetrate the prostatic capsule through the dorsolateral surface and supply the glandular tissues (Smith, 2008). The venous blood is drained by the prostatic vein into the internal iliac vein through the internal pudendal vein. The human prostate receives arterial blood from branches internal iliac artery, mainly from the inferior vesical artery (through the prostatic artery) but also from internal pudendal and middle rectal arteries (McMinn, 2003). Then, the blood is drained by the prostatic venous plexus located between the fibrous capsule of the prostate and the prostatic sheat and posteriorly drains into the internal iliac vein (Jacob, 2008; Cristini *et al*., 2013; Chatterjee *et al*., 2019). Arteries, veins, and nerve trunks can be recognized in the posterolateral region of the prostate within loose connective and adipose tissue (Kiyoshima, 2004) (Fig. 2).

Lymphatic drainage

Researchers are working to create novel metastatic animal models, but they lack a good understanding of lymphatic anatomy, which is essential to comprehend cancer metastasis (Suami *et al*., 2011). The knowledge about lymphatic drainage is crucial for the detection of sites of lymph node metastases. The sentinel node is defined as the first lymph node receiving lymph from the prostate (and consequently prostate tumors), and possibly developing the first metastases (Egawa *et al*., 2008). There are several differences and similarities between the lymphatic system of rat, dog, and human. The prostatic lymph vessels in rats drain into the medial iliac lymph nodes (Krinke, 2000). Compared to the body size difference between the human and the rat, there was little difference in the size of the lymphatic vessels between the two species (Wawroschek *et al*., 2003; Suami *et al*., 2022;). In dogs, the prostate drainage is performed through the iliosacral lymph
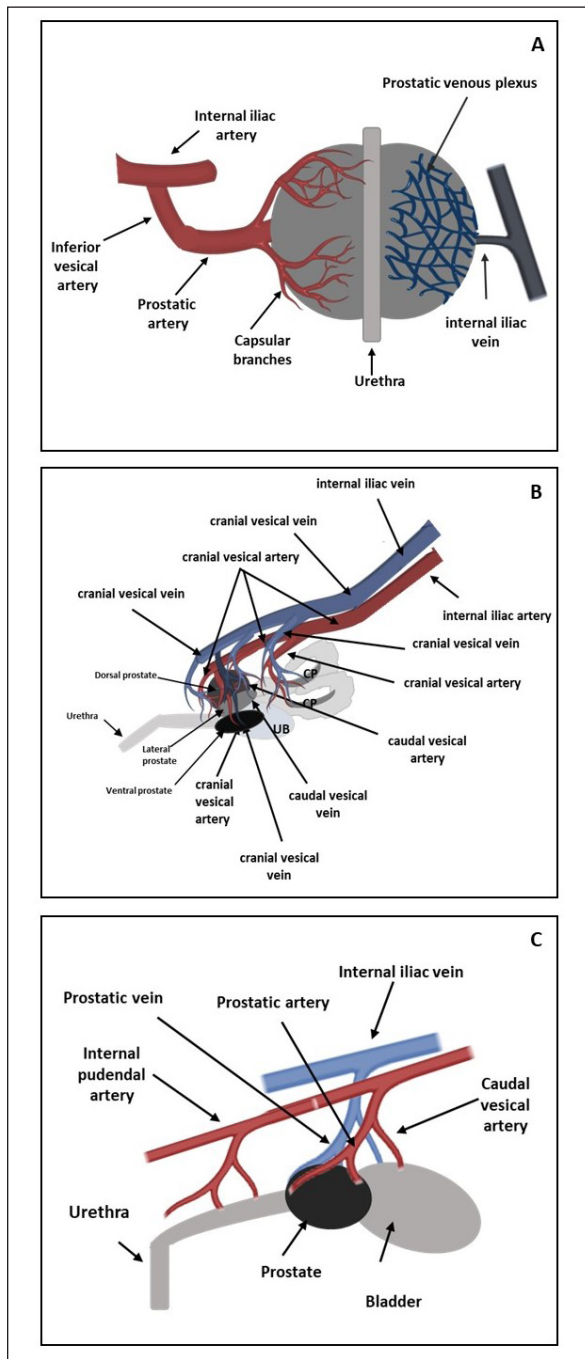
Fig. 2. Arterial supply (red) and venous drainage (blue) in human (A), rat (B) and dog (C) prostate gland. The figure was partly generated using Servier Medical Art, provided by Servier, licensed under a Creative Commons Attribution 3.0 unported license.

center through sacral and medial iliac lymph nodes (Suzuki *et al.*, 1992).

Regarding the lymphatic system in man, the main and important set of lymphatics course along the prostatic and internal iliac vessels and drain into the internal and common iliac lymph nodes and also the apex of the prostate gland into the sacral lymph nodes (Swanson and Hubbard, 2013; Boscolo-Berto *et al.*, 2020).

In the dog and in the man, different areas of the prostate have a variable drainage region, and the different lymphatic drainage of the periurethral and peripheral zone (PZ) is the only difference between the drainage of the human and canine prostate (Wawroschek *et al.*, 2003). Thus, the dog seems to be a good model to investigate prostatic lymphoscintigraphy.

Although still considered an experimental procedure for PCa, sentinel lymph node biopsy can be a better option for nodal staging, compared to extended pelvic lymph node dissection, especially given the heterogeneity of PCa and inconsistencies in definitions, types of tracer, descriptions of interventions, and detection methods (Mottet *et al.*, 2021; Lannes *et al.*, 2022). In an attempt to refine this procedure and translate the results to clinics, animals' models can be used. For example, Liss *et al.* (2014) used a canine model to investigate positron emission tomography/ computed tomography (PET/CT) preoperative imaging and intraoperative detection of a fluorescent-labeled receptor-targeted radiopharmaceutical. These authors concluded that this model has optimal logistic properties to obtain preoperative PET/CT and subsequent real-time intraoperative confirmation during robotic-assisted prostate sentinel lymph node dissection (Liss *et al.*, 2014). But there is a significant amount of interindividual variability in both canine and in human prostatic lymph drainage, which make it challenging to define the precise location of the sentinel lymph nodes (Wawroschek *et al.*, 2001, 2003). Wawroschek *et al.* (2001, 2003) suggested that in dogs the prostate sentinel lymph nodes are comparable to those in humans (Wawroschek *et al.*, 2003). Studies in men's prostate suggested that sentinel lymph nodes are located in the obturator region, external iliac, junctional, internal iliac, distal internal iliac, proximal internal iliac, common iliac, and in presacral regions (Wit *et al.*, 2017; Miki *et al.*, 2018; Narayanan and Wilson, 2018).

Prostate microscopic anatomy

In the rat, as already mentioned, the prostate is divided into four distinct lobes: the cranial, dorsal, lateral, and ventral prostate (VP) lobes. The cranial prostate lobe, also known as the coagulating gland, is a thin tubular structure attached to the seminal vesicles and follows its curvature (Hayashi *et al.*, 1991; Suwa *et al.*, 2001; Creasy *et al.*, 2012). The acini are tightly packed and are surrounded by smooth muscle and connective tissue attached to the seminal vesicles (Suwa *et al.*, 2001). The epithelium is cuboid to columnar with a degree of infoldings with possible cribriform patterns (Hayashi *et al.*, 1991; Suwa *et al.*, 2001; Creasy *et al.*, 2012). Secretory cells have round centrally located nuclei and

the cytoplasm is granular and eosinophilic (Creasy *et al.*, 2012). The stroma is composed of a connective tissue layer with a smooth muscle component (Suwa *et al.*, 2001). The dorsal prostate (DL) lobe has a butterfly shape and is located dorsally and bilaterally at the base of the seminal vesicles and behind the attachment of the cranial lobe (Hayashi *et al.*, 1991). The epithelium is simple and columnar, and cells have centrally located nuclei and the secretions are eosinophilic (Suwa *et al.*, 2001). The acini are large, with few infolding of the epithelium, and are loosely distributed within the stroma (Suwa *et al.*, 2001). Moreover, the acini are surrounded by stromal smooth muscle cells and fibrocytes (Creasy *et al.*, 2012) (Fig. 3). The LP lobe is located around the urethra, centrally and bilaterally, and is lined by a simple cuboid or tall columnar epithelium with very little infolding (Lee and Holland, 1987; Hayashi *et al.*, 1991; Creasy *et al.*, 2012). The acini are large and loosely in the stroma and the secretory cells have small and basal nuclei and the secretions are granular eosinophilic (Lee and Holland, 1987; Hayashi *et al.*, 1991; Suwa *et al.*, 2001; Creasy *et al.*, 2012). Sometimes, the dorsal and lateral lobes are referred to as the dorsolateral lobe due to the difficulty of anatomic separation of these lobes and similar histological features (Lee and Holland, 1987). The VP lobe wraps the urethra ventrally and is flanked by the two lobes that lay on both sides of the urethra (Hayashi *et al.*, 1991). The acini are composed of simple and columnar epithelium and the epithelial cells have base located nuclei without distinct nucleoli (Jesik *et al.*, 1982; Suwa *et al.*, 2001; Creasy *et al.*, 2012). The secretions in the acini are pale and slightly eosinophilic, and the stroma is thin (Lee and Holland, 1987; Creasy *et al.*, 2012). The glands show little amount of infolding and are surrounded by a thin fibromuscular layer (Hayashi *et al.*, 1991; Suwa *et al.*, 2001; Creasy *et al.*, 2012).

Each rat prostate lobe is composed of glands (acini) and a series of branching ducts that drain into the urethra (Lee *et al.*, 1990; Hayashi *et al.*, 1991). The glands are surrounded by smooth muscle cells that when they contract expel the prostate secretions (Lee and Holland, 1987). The stromal tissue of all lobes contains a mixture of elements that included extracellular material, small nerve endings, blood vessels, smooth muscle cells, fibroblasts, macrophages, and vascular endothelial cells (Jesik *et al.*, 1982; Lee and Holland, 1987; Prins *et al.*, 1991). Epithelial and luminal and basal cells are found in rat prostate and have different features (Prins *et al.*, 1991). Luminal cells express ARs and have a stronger reaction in the ventral prostate than in the dorsal and lateral lobes. Basal cells are ARs and α- and γ-actin negative in all prostate lobes and are intrinsically enriched in gene sets that are usually associated with stem cells. Prostate progenitor and stem cells are thought to reside within the basal layer and basal cells can give rise to luminal cells that are continually lost through apoptosis (Hu *et al.*, 2022).

On the other hand, in dogs, the prostate is involved by a fibromuscular capsule and is divided into the right and left lobes by a prominent medial septum (Sun *et al.*, 2017a; Cunto *et al.*, 2019), consisting of connective tissue and smooth muscle fibers (Cunto *et al.*, 2019). Each lobe is further divided into lobules separated by thin capsular trabeculae (Smith, 2008; LeRoy and Northrup, 2009; Cunto *et al.*, 2019). The lobules are organized into tubule-alveolar glands that are lined by tall columnar to cuboidal secretory epithelial cells (Fig. 3) (LeRoy and Northrup, 2009; Sun *et al.*, 2017a). The secretions leave these glands through a small duct that empties into the urethra near deferent ducts around the seminal colliculus (Smith, 2008; Sun *et al.*, 2017a; Cunto *et al.*, 2019). The luminal or secretory cells show abundant, granular, brightly eosinophilic cytoplasm when stained with hematoxylin and eosin (LeRoy and Northrup, 2009). Canine prostate-specific arginine esterase (CPSE), a serine protease similar to prostate-specific antigen (PSA), is the major secretory product of the dog prostate and is the most abundant protein in the dog's prostate fluid (Cunto *et al.*, 2019). CSPE can be used as a marker for prostate disorders (Alonge *et al.*, 2018). Moreover, these cells are positive
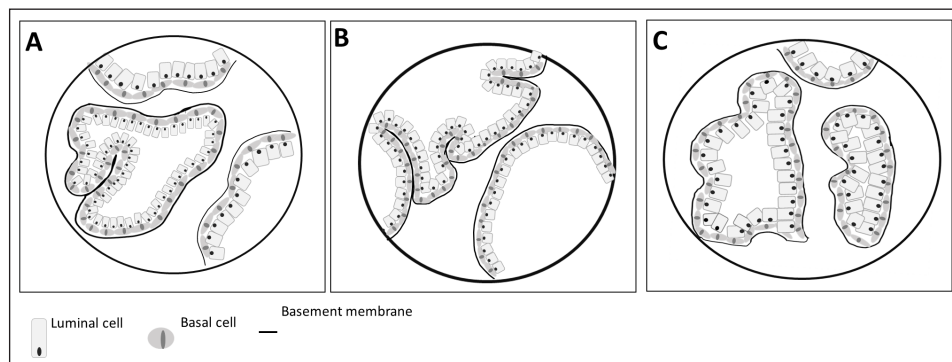

Fig. 3. Microscopic anatomy of the human prostate (A), dorsolateral prostate rat (B) and dog prostate (C).

for cytokeratin 8 and 18, NKX3.1, PTEN, and AR (Fonseca-Alves *et al*., 2013, 2018; Fernando Leis-Filho and Fonseca-Alves, 2019). The basal epithelial cells are located in the basal cell layer in a discontinuous pattern (LeRoy and Northrup, 2009; Sun *et al*., 2017a). Basal cells display expression of cytokeratin 5, high molecular weight cytokeratin, p63, and low expression of AR (Fonseca-Alves *et al*., 2018; Fernando Leis-Filho and Fonseca-Alves, 2019). The glandular tissue is supported by very thin septa of stroma composed of collagen fibers, fibroblasts, smooth muscle, and mononuclear inflammatory cells (Sun *et al*., 2017a). The basal layer also contains stem and progenitor cells (Bongiovanni *et al.*, 2019; Nascente *et al.* 2022)

In 1981, McNeal proposed a nomenclature to describe the structure of a human prostate, which is still used (McNeal, 1981). Therefore, the prostate contains distinct regions with different functions, and these are distinguished by their histological characteristics and anatomic pattern in PZ, central zone (CZ), transitional zone (TZ), and a periurethral gland or anterior fibromuscular stroma (AFMS) (McNeal, 1981; Selman, 2011; Bhavsar and Verma, 2014). Also, they have different susceptibility to pathological disorders (Lee *et al*., 2011). The PZ represents approximately 70% of the prostate volume and is located between the base and the apex along the posterior surface, surrounding the distal urethra (Lee *et al*., 2011; Bhavsar and Verma, 2014; Henry *et al*., 2018). The epithelium is simple, with small, rounded glands and composed of a single layer of columnar cells with basally located nuclei (Roy-Burman *et al*., 2004; Bhavsar and Verma, 2014). Moreover, PZ contains ductal and acinar elements with barely smooth muscle (Bhavsar and Verma, 2014). Most of the adenocarcinomas arise in PZ (Roy-Burman *et al*., 2004; Bhavsar and Verma, 2014; Sharma *et al*., 2017; Henry *et al*., 2018). The CZ is a cone-shaped structure located at the base of the prostate, between the peripheral and transition zones (Bhavsar and Verma, 2014). Representing approximately 25% of prostate volume, the CZ surrounds the ejaculatory ducts and extends from the neck of the bladder to the verumontanum (Roy-Burman *et al*., 2004; Bhavsar and Verma, 2014). The verumontanum is a structure located on the floor of the posterior urethra which marks the point where the ejaculatory ducts enter the urethra (Fine and Reuter, 2012; Bhavsar and Verma, 2014). The ducts and acini are larger than other zones and the epithelium has intraluminal ridges and a cribriform pattern (Aaron *et al*., 2016). A thin and compact layer of smooth muscle involves the gland making the epithelium appear crowded and pseudostratified with large polygonal glands (Roy-Burman *et al*., 2004; Bhavsar and Verma, 2014). The cells of this zone have darker granular cytoplasm, large nuclei and produce pepsinogen II, a major proteolytic enzyme of the seminal fluid (Roy-Burman *et al*., 2004; Sharma *et al*., 2017). This zone is described as having a low incidence of prostate disorders (Lee *et al*., 2011; Aaron *et al*., 2016). The TZ represents only 5% of the prostate volume and consists of two small lobes of glandular tissue which surround the proximal urethra between the bladder neck and the verumontanum (Roy-Burman *et al*., 2004; Bhavsar and Verma, 2014; Aaron *et al*., 2016). The epithelium is simple with small rounded glands, the secretory cells have pale cytoplasm and the stroma is dense with smooth muscle fibers (Roy-Burman *et al*., 2004; Bhavsar and Verma, 2014). TZ is the most common site for benign hyperplasia lesions and less commonly adenocarcinoma (De Marzo *et al*., 2007; Bhavsar and Verma, 2014). The AFMS represents less than 1% of the glandular prostate and forms the anterior surface of the prostate, and is located from PZ anterior to pre-prostatic urethra, extending from the apex to the base (Selman, 2011; Chatterjee *et al*., 2019). This zone is composed of connective tissue, smooth muscle, and some skeletal muscle with few glandular structures (Sharma *et al*., 2017; Chatterjee *et al*., 2019). Also, AFMS contains blood vessels that supply and drain the anterior prostate (Fine and Reuter, 2012). The prostate is composed of glandular and non-glandular (the stroma) elements within a capsule (Lee *et al*., 2011; Sharma *et al*., 2017). The existence of this capsule has been a controversial subject over the years, being considered more of an extension of the AFMS than a true capsule (Ayala *et al*., 1989; Roy-Burman *et al*., 2004; Bhavsar and Verma, 2014; Chatterjee *et al*., 2019). In 2004, a research paper analyzed 79 radical prostatectomy specimens and concluded that in 89% of the cases, the prostate capsule blends with the AFMS and forms the only anterior covering of the prostate (Kiyoshima, 2004). Also, in the majority of cases, AFMS connected and fused with lateral pelvic fascia and covers the outermost regions of the lateral and anterior surfaces of the prostate (Kiyoshima, 2004). The human prostate stroma is composed of smooth muscle cells (the most abundant cell type), fibroblasts, endothelial cells, infiltrating cells (like mast cells and lymphocytes), blood vessels, nerves, and stromal stem cells (Schalken, 2005; Prajapati *et al*., 2013; Ittmann, 2018). The muscle cell contractions will help the secretions enter into the urethra during ejaculation (Ross and Pawlina, 2006; Bhavsar and Verma, 2014). Stromal cells express mesenchymal markers such as CD34, vimentin, CD44, CD117, and CD90 (Takao and Tsujimura, 2008). Stromal stem cells have also been reported in the prostate stroma and have the function to replace and regenerate local cells that are destroyed due to injury or aging (Lin *et al*., 2007; Isaacs, 2008; Prajapati *et al*., 2013). These cells show high proliferative activity and the ability to differentiate into fibroblasts or smooth muscle cells and express mesenchymal stem cells markers, such as CD34 and Sca-1 (Lin *et al*., 2007; Prajapati *et al*., 2013). The

prostatic glands are composed of acini and ducts lined by different types of cells and are responsible for the production of seminal fluid. Luminal or secretory, basal, and neuroendocrine cells are the three major cell types, similar to rat and dog, but human prostate epithelium also has intermediate or amplifying cells and stem cells (Long *et al*., 2005; Adamowicz *et al*., 2017; Henry *et al*., 2018). The acini have a papillary appearance that is more visible in the CZ (Paner, 2016; Ittmann, 2018). The luminal cells are the most abundant cells, which are attached to the basal epithelial cells and extend into the acinar lumen (Fig. 3). The function of these cells is to secrete fluids to the lumen which contributes to the seminal fluid, such as the PSA and prostate acid phosphatase (Sharma *et al*., 2017; Ittmann, 2018). Moreover, these cells express cytokeratin 8 and 18, cell surface marker CD57, androgen-regulated secretory proteins (e.g. KLK3), AR, and estrogen receptor beta (ERβ) (Schalken, 2005; Di Zazzo *et al*., 2016; Henry *et al*., 2018). Their secretory capacity and viability are androgen dependent (Denmeade *et al*., 1996). Basal cells have a polygonal shape, large irregular-shaped nuclei, and a lack of secretory vesicles (Sharma *et al*., 2017). They are located between luminal cells and the underlying basement membrane and express cytokeratin 5 and 14, the transcription factor p63, Bcl1-2 (an anti-apoptotic factor), CD44, ERβ, and hepatocyte growth factor (Bonkhoff and Remberger, 1993; Di Zazzo *et al*., 2016; Sharma *et al*., 2017; Henry *et al*., 2018). Their function is the synthesis and secretion of the basement membrane components in these cells the AR are low or not expressed, which makes these cells independent of androgens for their survival (Sharma *et al*., 2017). Neuroendocrine cells are androgen-independent cells distributed all over the basal layer and don't express PSA (Schalken, 2005). There are two types of neuroendocrine cells: the open cells, with extensions at their apex that connect with the lumen, and closed cells, with dendritic processes that extend between adjacent cells located in the basal lamina and contact with the nerves (Vashchenko and Abrahamsson, 2005). Their function is cell growth, differentiation, and homeostatic regulation as well as regulation of prostatic secretion (Vashchenko and Abrahamsson, 2005). The major secretory products are chromogranin A, serotonin, bombesin, neuro-specific enolase, and calcitonin (Abrahamsson and Sant'agnese, 1993; Vashchenko and Abrahamsson, 2005). Intermediate or amplifying cells are proliferating cells that express basal and luminal markers, such as cytokeratin 8 or cytokeratin 5 (Long *et al*., 2005; Li and Shen, 2019). However, these cells raise the question of whether they can be considered a distinct cell type or just a transition between basal and luminal cells (Li and Shen, 2019). The prostate basal layer also contains a small heterogeneous population of stem cells, located mainly in the proximal region of the prostate ducts, near the urethra (Adamowicz *et al*., 2017; Leão *et al*., 2017; Li and Shen, 2019). The proliferation of these cells occurs when there are changes in the androgen levels triggered by physiology hormonal medium or by hormone therapy (Adamowicz *et al*., 2017). The markers used to identify these cells are CD133, CD44, ATP-binding cassette subfamily G member 2, telomerase reverse transcriptase, and CK5/CK14 (Mimeault *et al*., 2008; Prajapati *et al*., 2013; Adamowicz *et al*., 2017).

Conclusion

Animal models play a key role in biomedical research as they are used to test several therapies and drugs. However, translating the results obtained from these models into treatments for humans is a complex and controversial process. One of the most critical factors when selecting an animal model for biomedical trials is the degree of physiological and/or pathophysiological and anatomic similarity between the chosen species and humans. Selecting an inappropriate animal model for scientific research can lead to false results, waste of resources, and unnecessary harm to animal lives. Moreover, it can lead to inaccurate, redundant, and inappropriate trials. Therefore, a thorough understanding of the macroscopic and microscopic anatomy of the different animals used in experimentation is essential for obtaining results that can be translated into effective clinical outcomes for humans.

This review summarizes the major differences and similarities between rat, dog, and human prostate glands (Table 1). Dogs are considered by many researchers the best model to study PCa, due to the development of spontaneous cancer with a higher incidence when compared with other animals and the development of bone metastases. Moreover, although prostate tumors in dogs tend to be hormone insensitive and many of the tumors arise in castrated dogs, the fact that human and canine prostate glands share an embryologic origin and have many homologous anatomic and micro-anatomic structures suggests that they could serve as a model for human advanced castrate-resistant tumors. Anatomically, dog and human prostate share some characteristics. For example, the similarity in lymphatic system and the sentinel lymph node (Wawroschek *et al*., 2003). However, dogs have not been very used in experimental studies due to ethical reasons as they are commonly regarded as companion animals. But, dogs in animal experimentation aimed at helping humans have the potential to benefit not just humans, but also pet dogs themselves. Despite anatomical differences, the rats remain an important model to study human prostate diseases, once they share some features implicated in carcinogenesis with humans. Moreover, the rats are easy and cheap to maintain when compared with other species, and their physiology and genetics are well studied (Fagundes and Taha, 2004; Annon, 2020).

Table 1. Summary of the key anatomical features of the human, rat and dog prostate.

	Rat	Dog	Human
Anatomic localization	Caudal to the urinary bladder; incompletely surrounding the urethra	Surrounds the proximal urethra and the neck of urinary bladder.	Completely surrounds the proximal urethra
Lobes	Four lobes	Bilobed	Alobular structure
Shape	Not a compact organ	Ovoid	Conical
Microanatomy	Prostate surrounded by a thin mesothelial capsule; each lobe has glands and ducts	Two lobes within a fibromuscular capsule and each lobe is divided into lobules with tubule-alveolar glands	Ducts and glands in a compact organ within a pseudo-capsule
Epithelial cell types	Luminal and basal cells	Luminal and basal cells	Luminal or secretory, basal, neuroendocrine cells stem cells and intermediate or amplifying cells
Stroma	Sparse with minimal smooth muscle cells	Thin septa of stroma	Dense fibromuscular stroma
Stromal cell types	Smooth muscle cells, fibroblasts, macrophages, and vascular endothelial cells	Collagen fibers, fibroblasts, smooth muscle, and mononuclear inflammatory cells	Smooth muscle cells, fibroblasts, endothelial cells, infiltrating cells (like mast cells and lymphocytes), blood vessels, nerves, and stromal stem cells
Arterial supply	Branches of cranial vesical arteries (derived from internal iliac artery) supply cranial, dorsal, lateral, and ventral prostatic lobes; caudal vesical artery branch supply blood to the dorsal surface of prostate	Prostatic arteries (branches of the internal pudendal artery)	Prostatic arteries that are branches of the internal iliac artery (inferior vesical arteries, internal pudendal, and middle rectal arteries)
Venous drainage	Cranial and caudal vesical veins	Prostatic and urethral veins into the internal iliac vein	Prostatic venous plexus drains into the internal iliac veins
Lymphatic system	Medial iliac lymph nodes	Sacral and medial iliac lymph nodes	Internal iliac lymph nodes
Innervation	Postganglionar fibers derived from pelvic ganglion (innervated by both the hypogastric nerve and the viscerocutaneous branch of the pelvic nerve	Hypogastric nerve (sympathetic innervation) and pelvic nerve (parasympathetic control)	Parasympathetic innervation (arise from the pelvic splanchnic nerves) and sympathetic innervation (derived from the inferior hypogastric plexus)

Conflict of interest
The authors declare that they have no conflict of interest.

Author contributions
All Authors were responsible for manuscript writing and revision and approved its submission.

References

Aaron, L., Franco, O.E. and Hayward, S.W. 2016. Review of prostate anatomy and embryology and the etiology of benign prostatic hyperplasia. Urol. Clin. Am. 43(3), 279–288.

Abrahamsson, P.A. and Sant'agnese, P.A.D. 1993. Neuroendocrine cells in the human prostate gland. J. Androl. 14(5), 307–309.

Adamowicz, J., Pakravan, K., Bakhshinejad, B., Drewa, T. and Babashah, S. 2017. Prostate cancer stem cells: from theory to practice. Scand. J. Urol. 51(2), 95–106.

Alonge, S., Melandri, M., Leoci, R., Lacalandra, G.M. and Aiudi, G. 2018. Canine prostate specific esterase (CPSE) as an useful biomarker in preventive screening programme of canine prostate: CPSE threshold value assessment and its correlation with ultrasonographic prostatic abnormalities in asymptomatic dogs. Reprod. Domest. Anim. 53(2), 359–364.

Annon. 2020. Report from the commission to the European Parliament and the council. 2019 report on the statistics on the use of animals for scientific purposes in the Member States of the European Union in 2015-2017. Brussels, Germany: European Commission, p: 21.

Ayala, A.G., Ro, J.Y., Babaian, R., Troncoso, P. and Grignon, D.J. 1989. The prostatic capsule: does it exist? Its importance in the staging and treatment of prostatic carcinoma. Am. J. Surg. Pathol. 13(1), 21–27.

Bay, N.S.Y. and Bay, B.H. 2010. Greek anatomist herophilus: the father of anatomy. Anat. Cell. Biol. 43(4), 280–283.

Bhavsar, A. and Verma, S. 2014. Anatomic imaging of the prostate. Biomed. Res. Int. 2014, 9.

Biancardi, M.F., Dos Santos, F.C.A., de Carvalho, H.F., Sanches, B.D.A. and Taboga, S.R. 2017. Female prostate: historical, developmental, and morphological perspectives. Cell. Biol. Int. 41(11), 1174–1183.

Bongiovanni, L., Caposano, F., Romanucci, M., Grieco, V., Malatesta, D., Brachelente, C., Massimini, M., Benazzi, C., Thomas, R.E. and Salda, L.D. 2019. Survivin and Sox9: potential stem cell markers in canine normal, hyperplastic, and neoplastic canine prostate. Vet. Pathol. 56(2), 200–207.

Bonkhoff, H. and Remberger, K. 1993. Widespread distribution of nuclear androgen receptors in the basal cell layer of the normal and hyperplastic human prostate. Virchows. Arch. A. Pathol. Anat. Histopathol. 422(1), 35–38.

Boscolo-Berto, R., Siracusano, S., Porzionato, A., Polguj, M., Porcaro, A.B., Stecco, C., Macchi, V. and De Caro, R. 2020. The underestimated posterior lymphatic drainage of the prostate: an historical overview and preliminary anatomical study on cadaver. Prostate 80(2), 153–161.

Bosland, M.C. 1999. Use of animal models in defining efficacy of chemoprevention agents against prostate cancer. Eur. Urol. 35(5–6), 459–463.

Budras, K., McCarthy, P., Fricke, W., Richter, R., Horowitz, A. and Berg, R. 2007. Anatomy of the dog: an illustrated text, 5th ed. Hanover, Germany: Schluetersche.

Cekanova, M. and Rathore, K. 2014. Animal models and therapeutic molecular targets of cancer: utility and limitations. Drug. Des. Devel. Ther. 8, 1911–1921.

Chatterjee, A., Thomas, S. and Oto, A. 2019. Prostate MR: pitfalls and benign lesions. Abdom. Radiol. 45(7), 2154–2164.

Creasy, D., Bube, A., Rijk, E., de Kandori, H., Kuwahara, M., Masson, R., Nolte, T., Reams, R., Regan, K., Rehm, S., Rogerson, P. and Whitney, K. 2012. Proliferative and nonproliferative lesions of the rat and mouse male reproductive system. Toxicol. Pathol. 40(6_suppl.), 40S–121S.

Cristini, C., Pierro, G.B.D., Leonardo, C., Nunzio, C.D. and Franco, G. 2013. Safe digital isolation of the santorini plexus during radical retropubic prostatectomy. BMC. Urol. 13, 13.

Cunto, M., Mariani, E., Anicito Guido, E., Ballotta, G. and Zambelli, D. 2019. Clinical approach to prostatic diseases in the dog. Reprod. Domest. Anim. 54(6), 815–822.

De Marzo, A.M., Platz, E.A., Sutcliffe, S., Xu, J., Grönberg, H., Drake, C.G., Nakai, Y., Isaacs, W.B. and Nelson, W.G. 2007. Inflammation in prostate carcinogenesis. Nat. Rev. Cancer. 7(4), 256–269.

Denmeade, S.R., Lin, X.S. and Isaacs, J.T. 1996. Role of programmed (apoptotic) cell death during the progression and therapy for prostate cancer. Prostate 28(4), 251–265.

Di Zazzo, E., Galasso, G., Giovannelli, P., Di Donato, M., Di Santi, A., Cernera, G., Rossi, V., Abbondanza, C., Moncharmont, B., Sinisi, A.A., Castoria, G. and Migliaccio, A. 2016. Prostate cancer stem cells: the role of androgen and estrogen receptors. Oncotarget 7(1), 193–208.

Egawa, M., Fukuda, M., Takashima, H., Misaki, T., Kinuya, K. and Terahata, S. 2008. The sentinel node concept in prostate cancer: present reality and future prospects. Indian. J. Urol. 24(4), 451–456.

Evans, H.E. and Miller, M.E. 2013. Miller's anatomy of the dog, 4th ed. St. Louis, MO: Elsevier.

Fagundes, D.J. and Taha, M.O. 2004. Modelo animal de doença: critérios de escolha e espécies de animais de uso corrente. Acta. Cir. Bras. 19(1), 59–65.

Fernando Leis-Filho, A. and Fonseca-Alves, C.E. 2019. Anatomy, histology, and physiology of the canine prostate gland. In Veterinary anatomy and physiology. Eds., Rutland, C.S. and Kubale, V. London, UK: IntechOpen.

Fine, S.W. and Reuter, V.E. 2012. Anatomy of the prostate revisited: implications for prostate biopsy and zonal origins of prostate cancer: clinical implications of prostatic anatomy. Histopathology 60(1), 142–152.

Fonseca-Alves, C.E., Kobayashi, P.E. and Laufer-Amorim, R. 2018. Evaluation of NKX3.1 and C-MYC expression in canine prostatic cancer. Res. Vet. Sci. 118, 365–370.

Fonseca-Alves, C.E., Rodrigues, M.M.P., de Moura, V.M.B.D., Rogatto, S.R. and Laufer-Amorim, R. 2013. Alterations of C-MYC, NKX3.1, and E-cadherin expression in canine prostate carcinogenesis: C-MYC, NKX3.1, AND E-cadherin expression. Microsc. Res. Tech. 76(12), 1250–1256.

Ginja, M., Pires, M.J., Gonzalo-Orden, J.M., Seixas, F., Correia-Cardoso, M., Ferreira, R., Fardilha, M., Oliveira, P.A. and Faustino-Rocha, A.I. 2019. Anatomy and imaging of rat prostate: practical monitoring in experimental cancer-induced protocols. Diagnostics 9(3), 68.

Hayashi, N., Sugimura, Y., Kawamura, J., Donjacour, A.A. and Cunha, G.R. 1991. Morphological and functional heterogeneity in the rat prostatic gland. Biol. Reprod. 45(2), 308–321.

Henry, G.H., Malewska, A., Joseph, D.B., Malladi, V.S., Lee, J., Torrealba, J., Mauck, R.J., Gahan, J.C., Raj, G.V., Roehrborn, C.G., Hon, G.C., MacConmara, M.P., Reese, J.C., Hutchinson, R.C., Vezina, C.M. and Strand, D.W. 2018. A cellular anatomy of the normal adult human prostate and prostatic urethra. Cell. Rep. 25(12), 3530–3542.e5.

Hu, W.Y., Liu, L.F., Afradiasbagharani, P., Lu, R.L., Chen, Z.L., Hu, D.P., Birch, L.A. and Prins, G.S. 2022. Stem cells from a malignant rat prostate cell line generate prostate cancers *in vivo*: a model for prostate cancer stem cell propagated tumor growth. Am. J. Clin. Exp. Urol. 10(6), 377–389.

Isaacs, J.T. 2008. Prostate stem cells and benign prostatic hyperplasia. Prostate 68(9), 1025–1034.

Ittmann, M. 2018. Anatomy and histology of the human and murine prostate. Cold. Spring. Harb. Perspect. Med. 8(5), a030346.

Jacob, S. 2008. Chapter 4—Abdomen. In Human anatomy. Ed., Jacob, S. London, UK: Churchill Livingstone, pp: 71–123.

Jesik, C.J., Holland, J.M. and Lee, C. 1982. An anatomic and histologic study of the rat prostate. Prostate 3(1), 81–97.

Kiyoshima, K. 2004. Anatomical features of periprostatic tissue and its surroundings: a histological analysis of 79 radical retropubic prostatectomy specimens. Jpn. J. Clin. Oncol. 34(8), 463–468.

Krinke, G. 2000. The laboratory rat, 1st ed. Cambridge, MA: Academic Press.

Lannes, F., Baboudjian, M., Ruffion, A., Rouy, M., Giammarile, F., Rousseau, T., Kraeber-Bodéré, F., Rousseau, C., Rusu, D., Colombié, M., Brenot-Rossi, I., Rossi, D., Mottet, N. and Bastide, C. 2022. Radioisotope-guided lymphadenectomy for pelvic lymph node staging in patients with intermediate- and high-risk prostate cancer (The Prospective SENTINELLE Study). J. Urol. 209(2), 364–373.

Laufer-Amorim, R., Fonseca-Alves, C.E., Villacis, R.A.R., Linde, S.A.D., Carvalho, M., Larsen, S.J., Marchi, F.A. and Rogatto, S.R. 2019. Comprehensive genomic profiling of androgen-receptor-negative canine prostate cancer. Int. J. Mol. Sci. 20(7), 1555.

Leão, R., Domingos, C., Figueiredo, A., Hamilton, R., Tabori, U. and Castelo-Branco, P. 2017. Cancer stem cells in prostate cancer: implications for targeted therapy. Urol. Int. 99(2), 125–136.

Lee, C.H., Akin-Olugbade, O. and Kirschenbaum, A. 2011. Overview of prostate anatomy, histology, and pathology. Endocrinol. Metab. Clin. North. Am. 40(3), 565–575.

Lee, C. and Holland, J.M. 1987. Anatomy, histology, and ultrastructure (Correlation with function), prostate, rat. In Genital system. Eds., Jones, T.C., Mohr, U. and Hunt, R.D. Heidelberg, Germany: Springer Berlin Heidelberg, pp: 239–251.

Lee, C., Sensibar, J.A., Dudek, S.M., Hiipakka, R.A. and Liao, S. 1990. Prostatic ductal system in rats: regional variation in morphological and functional activities. Biol. Reprod. 43(6), 1079–1086.

LeRoy, B.E. and Northrup, N. 2009. Prostate cancer in dogs: comparative and clinical aspects. Vet. J. 180(2), 149–162.

Li, J.J. and Shen, M.M. 2019. Prostate stem cells and cancer stem cells. Cold. Spring. Harb. Perspect. Med. 9(6), a030395.

Lin, V.K., Wang, S.Y., Vazquez, D.V., Xu, C.C., Zhang, S. and Tang, L. 2007. Prostatic stromal cells derived from benign prostatic hyperplasia specimens possess stem cell like property. Prostate 67(12), 1265–1276.

Liss, M.A., Stroup, S.P., Qin, Z., Hoh, C.K., Hall, D.J., Vera, D.R. and Kane, C.J. 2014. Robotic-assisted fluorescence sentinel lymph node mapping using multimodal image guidance in an animal model. Urology 84(4), 982.e9–982.e14.

Long, R.M., Morrissey, C., Fitzpatrick, J.M. and Watson, R.W.G. 2005. Prostate epithelial cell differentiation and its relevance to the understanding of prostate cancer therapies. Clin. Sci. (Lond.) 108(1), 1–11.

McMinn, R.M.H. 2003. Last's anantomy: regional and applied, 9th ed. Chatswood, Australia: Elsevier Australia.

McNeal, J.E. 1981. The zonal anatomy of the prostate. Prostate 2(1), 35–49.

Miki, J., Yanagisawa, T., Tsuzuki, S., Mori, K., Urabe, F., Kayano, S., Yorozu, T., Sato, S., Kimura, T., Takahashi, H., Kishimoto, K. and Egawa, S. 2018. Anatomical localization and clinical impact of sentinel lymph nodes based on patterns of pelvic lymphatic drainage in clinically localized prostate cancer. Prostate 78(6), 419–425.

Mimeault, M., Mehta, P.P., Hauke, R. and Batra, S.K. 2008. Functions of normal and malignant prostatic stem/progenitor cells in tissue regeneration and cancer progression and novel targeting therapies. Endocr. Ver. 29(2), 234–252.

Mitterberger, M., Horninger, W., Aigner, F., Pinggera, G.M., Steppan, I., Rehder, P. and Frauscher, F. 2010. Ultrasound of the prostate. Cancer. Imaging. 10(1), 40–48.

Mottet, N., van den Bergh, R.C.N., Briers, E., Van den Broeck, T., Cumberbatch, M.G., De Santis, M., Fanti, S., Fossati, N., Gandaglia, G., Gillessen, S., Grivas, N., Grummet, J., Henry, A.M., van der Kwast, T.H., Lam, T.B., Lardas, M., Liew, M., Mason, M.D., Moris, L., Oprea-Lager, D.E., van der Poel, H.G., Rouvière, O., Schoots, I.G., Tilki, D., Wiegel, T., Willemse, P.M. and Cornford, P. 2021. EAU-EANM-ESTRO-ESUR-SIOG guidelines on prostate cancer-2020 update. Part 1: screening, diagnosis, and local treatment with curative intent. Eur. Urol. 79(2), 243–262.

Narayanan, R. and Wilson, T.G. 2018. Sentinel node evaluation in prostate cancer. Clin. Exp. Metastasis. 35(5), 471–485.

Nascente, E.D.P., Amorim, R.L., Fonseca-Alves, C.E. and de Moura, V.M.B.D. 2022. Comparative pathobiology of canine and human prostate cancer: state of the art and future directions. Cancers 14, 2727.

Nascimento-Gonçalves, E., Colaço, B., Ferreira, R. and Oliveira, P.A. 2019. Human and animal prostate cancer similarities and differences: models to study this disease. Prostate. Cancer. 17. Available via http://openaccessebooks.com/prostate-cancer.html#X

Nascimento-Gonçalves, E., Faustino-Rocha, A.I., Seixas, F., Ginja, M., Colaço, B., Ferreira, R., Fardilha, M. and Oliveira, P.A. 2018. Modelling human prostate cancer: rat models. Life. Sci. 203, 210–224.

Nascimento-Gonçalves, E., Ferreira, R., Oliveira, P.A. and Colaço, B.J.A. 2020. An overview of current alternative models for use in the context of prostate cancer research. Altern. Lab. Anim. 48(2), 58–69.

Oliveira, D.S.M., Dzinic, S., Bonfil, A.I., Saliganan, A.D., Sheng, S. and Bonfil, R.D. 2016. The mouse prostate: a basic anatomical and histological guideline. Bosn. J. Basic. Med. Sci. 16(1), 8–13.

Palmer, R. 1981. Nicolò Massa, his family and his fortune. Med. History. 25(4), 385–410.

Paner, G. 2016. Prostate gland and seminal vesicle. Diagnostic pathology: genitourinary, 2nd ed. Elsevier, pp: 4–165.

Pinho, S.S., Carvalho, S., Cabral, J., Reis, C.A. and Gärtner, F. 2012. Canine tumors: a spontaneous animal model of human carcinogenesis. Transl. Res. 159(3), 165–172.

Prajapati, A., Gupta, S., Mistry, B. and Gupta, S. 2013. Prostate stem cells in the development of benign prostate hyperplasia and prostate cancer: emerging role and concepts. Biomed. Res. Int. 2013, 107954.

Ross, M. and Pawlina, W. 2006. Male reproductive system. Histology, a text and atlas, 5th ed. Philadelphia, PA: Lippincott Williams, pp: 728–771.

Prins, G.S., Birch, L. and Greene, G.L. 1991. Androgen receptor localization in different cell types of the adult rat prostate. Endocrinology 129(6), 3187–3199.

Roy-Burman, P., Wu, H., Powell, W.C., Hagenkord, J. and Cohen, M.B. 2004. Genetically defined mouse models that mimic natural aspects of human prostate cancer development. Endocr. Relat. Cancer. 11(2), 225–254.

Sanches, B.D.A., Zani, B.C., Maldarine, J.S., Biancardi, M.F., Santos, F.C.A., Góes, R.M., Vilamaior, P.S.L. and Taboga, S.R. 2016. Postnatal development of Mongolian gerbil female prostate: an immunohistochemical and 3D modeling study. Microsc. Res. Tech. 79(5), 438–446.

Schalken, J. 2005. Androgen receptor mediated growth of prostate (Cancer). Eur. Urol. Suppl. 4(8), 4–11.

Seeley, R., Stephens, T. and Tate, P. 2004. Anatomy and physiology, 6th ed. New York, NY: The McGraw-Hill.

Selman, S.H. 2011. The McNeal prostate: a review. Urology 78(6), 1224–1228.

Shappell, S.B., Thomas, G.V., Roberts, R.L., Herbert, R., Ittmann, M.M., Rubin, M.A., Humphrey, P.A., Sundberg, J.P., Rozengurt, N., Barrios, R., Ward, J.M. and Cardiff, R.D. 2004. Prostate pathology of genetically engineered mice: definitions and classification. The consensus report from the bar harbor meeting of the mouse models of Human Cancer Consortium Prostate Pathology Committee. Cancer. Res. 64(6), 2270–2305.

Sharma, M., Gupta, S., Dhole, B. and Kumar, A. 2017. Anatomical, development and genetic basis of maleness. Basics of human andrology: a textbook. Springer, pp: 536.

Shirai, T., Takahashi, S., Cui, L., Futakuchi, M., Kato, K., Tamano, S. and Imaida, K. 2000. Experimental prostate carcinogenesis—rodent models. Mutat. Res. 462(2–3), 219–226.

Smith, J. 2008. Canine prostatic disease: a review of anatomy, pathology, diagnosis, and treatment. Theriogenology 70(3), 375–383.

Standring, S. 2020. Gray's anatomy: the anatomical basis of clinical practice. Edinburgh, UK: Elsevier Health Sciences.

Suami, H., Chang, D.W., Matsumoto, K. and Kimata, Y. 2011. Demonstrating the lymphatic system in rats with microinjection. Anat. Rec. (Hoboken). 294(9), 1566–1573.

Sun, F., Báez-Díaz, C. and Sánchez-Margallo, F.M. 2017a. Canine prostate models in preclinical studies of minimally invasive interventions: Part I, canine prostate anatomy and prostate cancer models. Transl. Androl. Urol. 6(3), 538–546.

Sun, F., Báez-Díaz, C. and Sánchez-Margallo, F.M. 2017b. Canine prostate models in preclinical studies of minimally invasive interventions: Part II, benign prostatic hyperplasia models. Transl. Androl. Urol. 6(3), 547–555.

Sung, H., Ferlay, J., Siegel, R.L., Laversanne, M., Soerjomataram, I., Jemal, A. and Bray, F. 2021. Global cancer statistics 2020: GLOBOCAN estimates of incidence and mortality worldwide for 36 cancers in 185 countries. CA. Cancer. J. Clin. 71(3), 209–249.

Suwa, T., Nyska, A., Peckham, J.C., Hailey, J.R., Mahler, J.F., Haseman, J.K. and Maronpot, R.R. 2001. A retrospective analysis of background lesions and tissue accountability for male accessory sex organs in Fischer-344 rats. Toxicol. Pathol. 29(4), 467–478.

Suzuki, T., Kurokawa, K., Yamanaka, H. and Jimbo, H. 1992. Lymphatic drainage of the prostate gland in canines. Prostate 21(4), 279–286.

Swanson, G.P. and Hubbard, J.K. 2013. A better understanding of lymphatic drainage of the prostate with modern imaging and surgical techniques. Clin. Genitourin. Cancer. 11(4), 431–440.

Takao, T. and Tsujimura, A. 2008. Prostate stem cells: the niche and cell markers. Int. J. Urol. 15(4), 289–294.

Vashchenko, N. and Abrahamsson, P.A. 2005. Neuroendocrine differentiation in prostate cancer: implications for new treatment modalities. Eur. Urol. 47(2), 147–155.

Wawroschek, F., Vogt, H., Weckermann, D., Wagner, T., Hamm, M. and Harzmann, R. 2001. Radioisotope guided pelvic lymph node dissection for prostate cancer. J. Urol. 166(5), 1715–1719.

Wawroschek, F., Wengenmair, H., Senekowitsch-Schmidtke, R., Hamm, M., Henke, J., Schönberger, T., Hauser, A., Erhardt, W. and Harzmann, R. 2003. Prostate lymphoscintigraphy for sentinel lymph node identification in canines: reproducibility, uptake, and biokinetics depending on different injection strategies. Urol. Res. 31(3), 152–158.

Wit, E.M.K., Acar, C., Grivas, N., Yuan, C., Horenblas, S., Liedberg, F., Valdes Olmos, R.A., van Leeuwen, F.W.B., van den Berg, N.S., Winter, A., Wawroschek, F., Hruby, S., Janetschek, G., Vidal-Sicart, S., MacLennan, S., Lam, T.B. and van der Poel, H.G. 2017. Sentinel node procedure in prostate cancer: a systematic review to assess diagnostic accuracy. Eur. Urol. 71(4), 596–605.